Lab on a Chip

Cite this: *Lab Chip*, 2012, **12**, 2995–2997

www.rsc.org/loc

HIGHLIGHT

Research highlights

Šeila Selimović,[ab] Cole A. DeForest,[c] Mehmet R. Dokmeci[ab] and Ali Khademhosseini*[abde]

DOI: 10.1039/c2lc90080g

Nanofluidic channels by electron-beam-induced etching

There is a growing interest in developing processing techniques to create materials with user-defined nanoscopic features. With their unique transport properties and enabling studies of physical phenomena that are often overlooked by larger-scale systems, nanofluidic structures have applications in chemical sensors, biotechnology, and electronics.[1] Although a variety of methods have been developed to create these devices (*e.g.*, photolithography, femtosecond laser machining, and micromolding), electron beam (e-beam) lithography remains the method of choice in the creation of planar devices with well-defined width and depth features of sub-100 nm. With the advances in next-generation fabrication technologies, substantial efforts are being devoted towards those that enable finer resolution (*i.e.*, smaller features) and custom designed 3D geometry.

Recently, Jacobson and colleagues have combined e-beam lithography with an electron-beam-induced etching (EBIE) processing technique to create nanomaterials with highly precise 3D geometry and increased resolution.[2] While e-beam lithography was used to write portions of the substrate directly and selectively by bombarding the monomer material with high-energy electrons, EBIE was used as a chemical etching strategy that relied on the dissociation of a precursor gas (typically XeF_2 or H_2O) locally by an e-beam. The disassociated gas then reacted with the substrate surface and created a volatile intermediate by-product that desorbed from the surface and etched the material, resulting in finer feature sizes. The feature geometry and the size scale of the devices can be directly dictated by the user by changing the electron acceleration potential, current density, and other parameters.

Perry *et al.* demonstrated the utility of this approach by first generating μm wide lines of SU-8, a common negative-tone photoresist. Areas of 1 μm × 1 μm were then etched into the SU-8 lines by EBIE. A linear relationship between etch depth, quantified by AFM measurements, and e-beam dosage was observed over a range of acceleration potentials (~kV), with typical depths ranging between 50 and 200 nm. The linear correlation between material removal and e-beam dose was highly reproducible over the ~2 year timeframe in which the experiments were performed, enabling EBIE to be used in a predictable fashion to generate desired patterns.

Since the etch rate depended on the amount of exposed surface area present, the sharp edges initially generated through e-beam lithography were transformed into smooth features in a predictable manner. Moreover, since the etching was initiated locally, EBIE provided a means to control 3D structures in the form of localized thickness within the material. For a given acceleration potential and gas pressure, increased EBIE modification times (a few sec) resulted in decreased feature height (150–60 nm) and sample width near the region of e-beam focusing. Moreover, e-beam-generated nanofunnel structures could be reduced in size by EBIE by a factor of 0.5 (Fig. 1), while maintaining the 3D shape of the features. Replicas of these nanofunnels were fabricated by casting high-modulus poly(dimethylsiloxane) (h-PDMS) onto masters and excellent pattern transfer was observed.

By combining e-beam lithography with EBIE postprocessing, Jacobson and colleagues were able to generate 3D nanoscale structures with high precision while simultaneously decreasing the feature size obtainable by standard technologies. As this approach is further developed and applied to higher-resolution initial features, we expect that it could be used to extend the limits of obtainable feature sizes and to generate structures that provide new and unique applications in a variety of fields.

A point-of-care flu detection chip

Despite advances in medical diagnostics and treatment, the influenza virus is responsible for several hundred thousand hospitalizations and over 50 000 deaths every year in the United States alone.

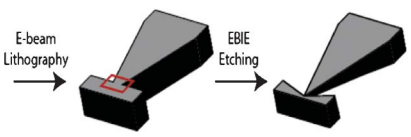

Fig. 1 Features generated with e-beam lithography were processed with focused EBIE modification (red box), resulting in a localized decrease in feature width and thickness. Image inspired by data from Perry *et al.*[2]

[a]*Center for Biomedical Engineering, Department of Medicine, Brigham and Women's Hospital, Harvard Medical School, Cambridge, Massachusetts 02139, USA. E-mail: alik@rics.bwh.harvard.edu*
[b]*Harvard-MIT Division of Health Sciences and Technology, Massachusetts Institute of Technology, Cambridge, Massachusetts 02139, USA*
[c]*Division of Chemistry and Chemical Engineering, California Institute of Technology, Pasadena, California 91125, USA*
[d]*Wyss Institute for Biologically Inspired Engineering, Harvard University, Boston, Massachusetts 02115, USA*
[e]*World Premier International – Advanced Institute for Materials Research (WPI-AIMR), Tohoku University, Sendai 980-8577, Japan*

Moreover, new strains develop continuously, with types like influenza A or H1N1 reaching pandemic levels and causing tens of thousands of deaths.[3] A treatment for the influenza disease is difficult to implement, as the virus mutates quickly. Hence, research efforts are being focused on rapid, early and accurate detection.

For a diagnostic device to be efficient – yield accurate results with high specificity and reach a large number of patients – it should be designed as a point-of-care device. That is, it should be affordable and simple to integrate into existing medical laboratories. Klapperich and colleagues have recently introduced a prototype device, combining microfluidic principles with polymerase chain reaction (PCR) for rapid testing of human nasopharyngeal samples.

The microfluidic device developed by Cao *et al.*[4] was fabricated from a thermoplastic polymer and sealed with a flat slab of the same material. Using a thermoplastic ensured a low cost per chip and the fabrication technology was amenable to high-volume, industrial production. The simple fluidic structure consisted of a straight sample preparation channel containing a porous, solid column for nucleic acid extraction, a wide channel for reverse transcription (RT) and a serpentine channel for PCR (Fig. 2). The column material contained a mixture of methacrylates, a photoinitiator and silica microbeads. It was injected into the sample preparation channel and solidified under UV-light. Thus, a setup for nucleic acid extraction was easily reduced from the benchtop scale to the microfluidic scale. Similarly, PCR was enabled on-chip by engineering a long, serpentine channel that was positioned on top of two metal heaters. As the sample flowed through this channel, it passed 30 times between a 60 °C (annealing) and 95 °C (denaturation) region.

Samples were collected by swabbing of, or aspirating from, the nasopharyngeal cavities of 146 patients. Since the chip was designed for single use, a different chip could be utilized for testing each sample. These samples (on the order of 100 μl) were first centrifuged to remove debris, then mixed with a lysis buffer and were ran through the column. The collected RNA was washed to purify the solution. In the second step, enzymes for RT were added to the sample on-chip for an incubation period of 45 min at a high temperature (above 50 °C). Here, the small number of collected RNA molecules were reverse transcribed into the corresponding DNA complements. To increase the yield, the sample was then transported into the PCR channel. At the end of the PCR channel, the amplified RNA was collected and evaluated using gel capillary electrophoresis – the only procedure that was conducted off-chip.

The microfluidic test was sufficiently sensitive to detect as few as 1000 viruses/ml, in both swabs and aspirates. The percentage of correctly identified positives (sensitivity) was 96%, and negatives (specificity) was 100%. These values are comparable to the more complex method of direct fluorescent antigen testing, but much more reliable than benchtop rapid tests (with ~50% sensitivity). Furthermore, the RNA extraction and amplification required a period of only 3 h, while highly reliable viral cultures require much longer time periods.

The microfluidic chip presented here is noteworthy for its advantages over standard benchtop testing methods. It is highly precise, fast, portable, and cost-efficient. These are all characteristics that make this chip a likely candidate to be widely used as a point-of-care influenza detection device. However, to make the chip even more appealing to the end-users (medical technicians), it should be packaged together with an analysis platform, *e.g.* one based on electrophoresis, and be able to distinguish between different influenza strains. Such a chip would greatly advance public health efforts in early stage tracking and containing outbreaks of new viral strains.

A microfluidic study of drug transport in tumors

Developing new, efficient cancer treatments involves efforts in, among others, drug screening and *in vitro* studies of tumor tissues.[5] Before new cancer drugs can be administered to patients, extensive tissue culture and animal testing is required. Engineered tissues have started to become interesting drug testing platforms. Such 3D laboratory-grown tissues,

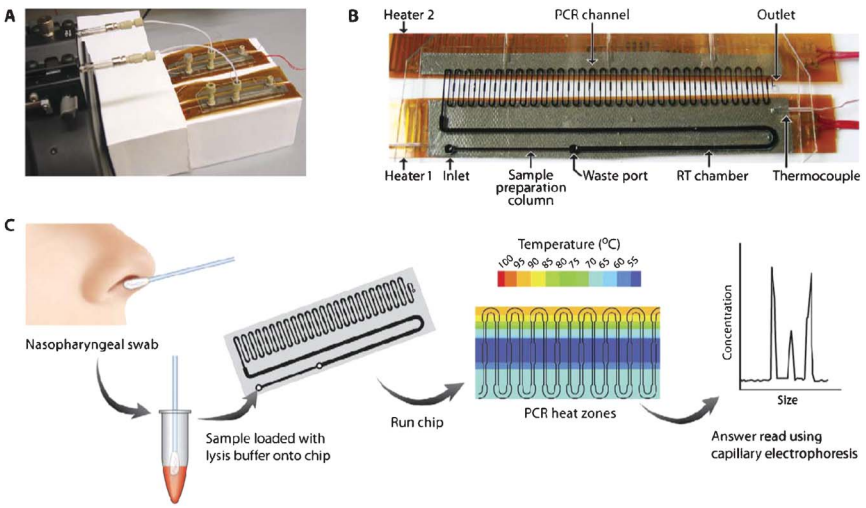

Fig. 2 A) Two testing chips, connected *via* tubing to a syringe pump. B) A magnified image of the microfluidic chip, showing different functional elements. C) Sketch of the sample testing procedure. Image reprinted with permission from Cao *et al.*[4]

however, tend to be non-uniform in cell distribution and are therefore not always an appropriate representative of the real tumors. However, a close approximation of the density and uniformity of the real cancerous tissue is particularly important, as these parameters can affect the distribution of drugs in solid tumors. For example, the low efficacy of certain chemotherapies has been attributed to the limited transport of drugs inside a tumor.[6]

To develop more uniform 3D tumor models, Elliott and Yuan[7] have recently explored a microfluidic approach to *in vitro* seeding of cancer cells. Their poly (dimethylsiloxane) (PDMS)–glass device consisted of two parallel outer channels and one 100 μm wide inner channel situated between them. The three channels were connected *via* an array of 4 μm wide capillary paths. The outer channels were primed with collagen, then the device was saturated with phosphate buffered saline inside a bath. This would later prevent evaporation of the aqueous sample. Mouse melanoma cells were introduced into the inner channel at a concentration of a few million/ml. The cells could not pass through the capillary paths without an added external pressure, but medium and later drug solutions could flow freely between the outer and inner channels. Thus, the cells were confined to and uniformly distributed inside the inner channel, which was demonstrated by staining the cell nuclei. The cells were continuously perfused for a culture period of 12 h.

While the measured cell packing density was reduced by a third at the end of the culture, it was comparable to the values for *in vivo* tumors. Also, during the 12 h, the cell nuclei became larger and elongated. In addition, the individual cells could not be removed by increasing the flow rate, indicating that the cells had formed a single cohesive construct.

To mimic the transport of a drug in this tissue, Elliott and Yuan introduced sodium fluorescein (NaF) into the outer channels and observed its permeation into the inner channel. The transport behavior of the molecule was quantified in terms of the mean and maximum dye intensity (I_{mean}/I_{max}). This molecule could not penetrate the cell membrane, but could only pass through the extracellular space. The farthest permeation into the inner channel corresponded to the seeded cell suspension containing collagen. The protein prevented the cells from attaching to each other, thereby increasing the space between them and allowing the NaF to pass unobstructed. Similar results were observed immediately after loading of a pure cell suspension. At this point the cells had not yet fused together, enabling free movement of the NaF dye. However, at the end of this culture, an opposite trend was observed. Here, the cohesive cell structure hindered the transport of the dye. Importantly, the permeation behavior was consistent along the length of the inner channel, further strengthening the observation that cell distribution was uniform in this model.

Numerical simulations of the 2D NaF diffusion matched well with the experimental results. A mathematical model identified the following chief variables in controlling the transport behavior: the duration of the experiment (observation time), channel width (transport distance) and the relative resistance of the inner channel and the capillary paths to diffusion. Understanding the underlying mechanism for molecular diffusion in dense tissue, and thus being able to simulate the system numerically could be helpful during the drug screening process. Namely, drugs that permeate cancerous tissue poorly could be identified early using a numerical model and eliminated from the screening tests.

An aberration from the numerical prediction was observed when the diffusing molecule was membrane-permeable, such as Hoechst 33342 (a nucleus stain). This dye was strongly absorbed by the cells, leaving few molecules free to diffuse through the interstitial space. This particular result could potentially explain why some small anti-cancer drugs only weakly penetrate solid tumors.

Another insight that this microfluidic device offered was related to the permeation of calcein acetoxymethyl ester, which is commonly used to stain live cells. Similar to the Hoechst dye, this molecule did not penetrate far into the inner channel. However, after conducting control experiments off-chip, the researchers hypothesized that the lack of penetration was not due to strong cellular uptake, but due to the expression of proteins responsible for multidrug resistance. Thus, this particular study offered information which could not be provided in benchtop experiments.

The examples listed here clearly demonstrate the usefulness of this microfluidic chip for studies on cell–drug interactions, drug delivery and, in particular, for testing novel cancer drugs. The chip enabled uniform, high-density seeding of cells and thus the rapid engineering of uniformly dense solid tumors. In addition to these important biological achievements, the present research is noteworthy for its creative application of a simple fluidic structure to a project that could potentially yield a variety of powerful, sophisticated results.

References

1 R. B. Schoch, J. Y. Han and P. Renaud, *Rev. Mod. Phys.*, 2008, **80**, 839–883.
2 J. M. Perry, Z. D. Harms and S. C. Jacobson, *Small*, 2012, **8**, 1521–1526.
3 N. M. Scalera and S. B. Mossad, *Postgrad. Med.*, 2009, **121**, 43–47.
4 Q. Cao, M. Mahalanabis, J. Chang, B. Carey, C. Hsieh, A. Stanley, C. A. Odell, P. Mitchell, J. Feldman, N. R. Pollock and C. M. Klapperich, *PLoS One*, 2012, **7**, e33176.
5 K. M. Yamada and E. Cukierman, *Cell*, 2007, **130**, 601–610.
6 M. R. Dreher, W. Liu, C. R. Michelich, M. W. Dewhirst, F. Yuan and A. Chilkoti, *J. Natl. Cancer Inst.*, 2006, **98**, 335–344.
7 N. T. Elliott and F. Yuan, *Biotechnol. Bioeng.*, 2012, **109**, 1326–1335.